International Journal of Data Analysis and Information Systems
VOLUME 10 • NUMBER 1 • JUNE 2018

A Sensitive Structure based on ZnO-rGO Nanocomposite with Remarkably Enhanced Visible-light-driven Photoresponse Performance

Xiaoliang Yea*
[a] *School of Electronics Information, Shanghai Dianji University, Shanghai 200240, China*

ABSTRACT

Zinc oxide-reduced graphene oxide (ZnO-rGO) nanocomposite has been successfully developed in this work. The photoelectric sensitive structures based on ZnO and ZnO-rGO nanocomposite with enhanced photoelectric response under white irradiation were demonstrated. The currents of photoelectric sensitive structures based on ZnO NWs and ZnO-rGO nanocomposite were recorded separately under UV and visible light illumination. The photocurrent of device based on ZnO-rGO nanocomposite under white irradiation is close to one order of magnitude greater than its counterpart based on ZnO nanowires. The deviece based on ZnO-rGO nanocomposite is also characterized by an excellent stability and reproducibility. The photoelectric sensitive structure based on ZnO-rGO nanocomposite may have a potential application in visible light devices.

Keywords: Semiconductor, Zinc oxide, Nanocomposite, Device

1. INTRODUCTION

ZnO, as a semiconducting material with wide direct band gap (3.37 eV) and large exciton binding energy (60 meV), has been widely used in ultraviolet (UV) laser diodes, UV optical detectors, piezoelectric devices, solar cells, etc [1-3]. Different kinds of ZnO nanostructures, such as nanorod, nanowire, nanotube and nanobelt have been reported [4-7]. Especially, ZnO nanowires (NWs) have attracted special attention because of their great potential in terms of optical devices. However, the weak responsivity of pure ZnO greatly hinders its practical application due to the fast recombination of photogenerated electron and hole pairs in the single phase semiconductor [8-10]. It is necessary to improve the photoresponse of structure based on pure ZnO, which is often enhanced by doping ion or combining with other electron-accepting materials [11-13].

Graphene, a unique two-dimensional structure of sp2 carbon atom arranged in a honeycomb-like lattice, has attracted considerable interest due to its fascinatingly electronic and mechanic properties. The combination of graphene and ZnO can exhibit excellent optoelectronic properties by improving the carrier transport and collection efficiency. At present, some different preparation methods and applications for ZnO-graphene composite have been reported. For example, D. L. Shao reported ZnO quantum dots combined with graphene using atomic layer deposition method [14]. Huynh Ngoc Tien showed a ZnO-graphene sphere composite through a solvothermal reaction mathed [15]. Kumar et al. demonstrated PL properties of ZnO-graphene multipod composite by a hydrothermal method [16]. However, up to now, it is limited that the study of ZnO-rGO nanostructure under visible light irradiation. Moreover, a low bias of 1 V will be applied and investigated in our work, which is more meaningful because of easily applied advantages in practice [17,18].

In this study, the photoelectric sensitive structure based on ZnO-rGO nanocomposite has been prepared through a chemical vapor deposition (CVD) with a microfabrication procedure. The photoelectric response of device based on ZnO-rGO with a low bias voltage was investigated under white light source. The current values of photoelectric sensitive structures based on ZnO NWs and ZnO-rGO nanocomposite were recorded under UV and visible light illumination. Compared with the device based on ZnO NWs under UV illumination, the sensitive structure based on ZnO-rGO nanocomposite under

white irradiation shows dramatically stronger photoresponse performances than under UV illumination. Meanwhile, the charge transfer process between the ZnO NWs and the rGO sheet under visible irradiation was also discussed.

2. EXPERIMENTAL

The ZnO NWs were synthesized via a chemical vapor deposition technique and the rGO sheet was prepared by the modified Hummers method in our previous reports [19,20]. The interdigitated electrodes were made by sputtering 50 nm Ti and 170 nm Au onto a patterned photoresist mold. The dissolved ZnO and ZnO-rGO nanocomposite with ethanol solution were deposited on between electrodes and the networks of devices based on ZnO and ZnO-rGO would be formed. The morphology of ZnO-rGO nanocomposite was characterized by scanning electron microscope (SEM, Zeiss Ultra 55, Germany) and the elemental composition measurement was carried out by energy dispersive spectroscopy (EDS). The crystal structure of as-prepared ZnO-rGO sample was tested using an advanced X-ray diffractometer (D8 ADVANCE, Bruker, Germany). The UV-vis absorption spectral measurement was performed using a UV-Vis spectrophotometer. Current-voltage characteristics of the fabricated devices were monitored using Agilent 4156C at room temperature.

3. RESULTS AND DISCUSSION

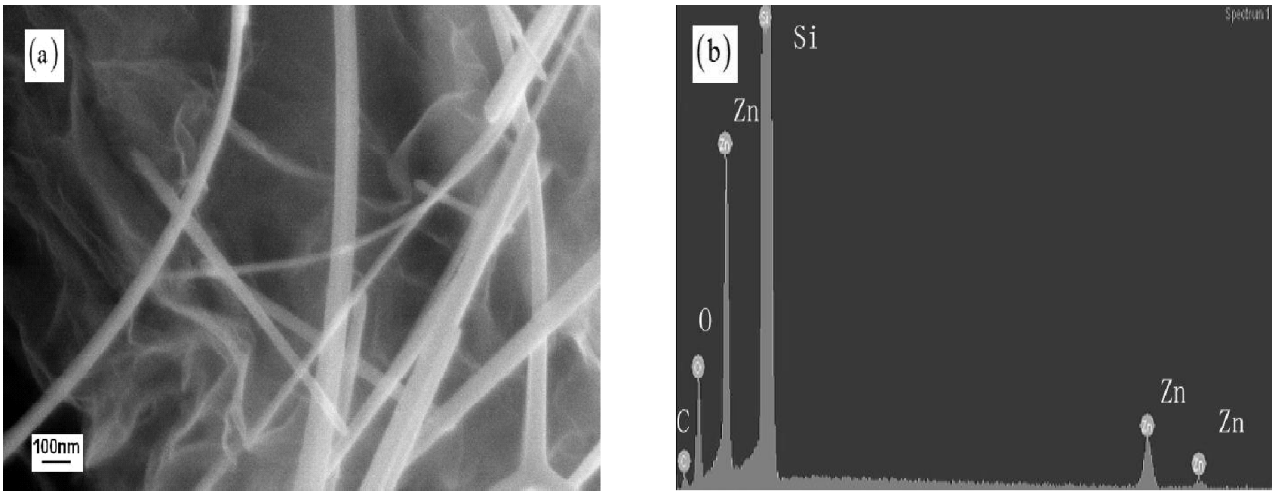

Figure 1: (a) The SEM image of ZnO-rGO nanocomposite. (b) The EDS pattern of a ZnO-rGO nanocomposite

Fig. 1 (a) shows a typical scanning electron microscope (SEM) image of the the prepared sample. The morphology reveals the shape of ZnO-rGO sample. The average diameter of NWs was estimated to be approximately 40 nm. After hybridization of ZnO nanowires with rGO sheets, it can be seen that the nanocomposite was made up with rGO sheets and ZnO NWs. Fig. 1(b) presents the energy dispersive X-ray spectroscopy (EDS) pattern for the ZnO-rGO nanocomposite. It clearly indicates the existence of Zn and C atoms originated from the ZnO and rGO, respectively. This result confirms the successful formation of ZnO-rGO hybrid structure.

Fig. 2 (a) shows the XRD pattern of ZnO-rGO nanocomposite. A series of diffraction peaks at 31.81°, 34.48°, 36.33°, 47.59°, 56.64°, 63.08°, 64.41°, 67.98° and 69.14°, corresponding to (100), (002), (101), (102), (110), (103), (200), (112) and (201) planes of hexagonal wurtzite ZnO structure, can be observed. The diffraction peaks of ZnO-rGO nanocomposite are similar to those of hexagonal phase wurtzite ZnO. The broad diffraction band ranging from 20æ%to 30æ% is observed in ZnO-rGO nanocomposite, which are likely to be defects connected with rGO during chemical reduction process. Fig. 2 (b) shows the UV-vis absorption spectra spectra of ZnO NWs and ZnO-rGO nanocomposite. The two samples show a similar absorption peak at 375nm. The ZnO-rGO nanocomposite exhibits a stronger absorbance than the ZnO NWs within the range of 300 nm and 800 nm.

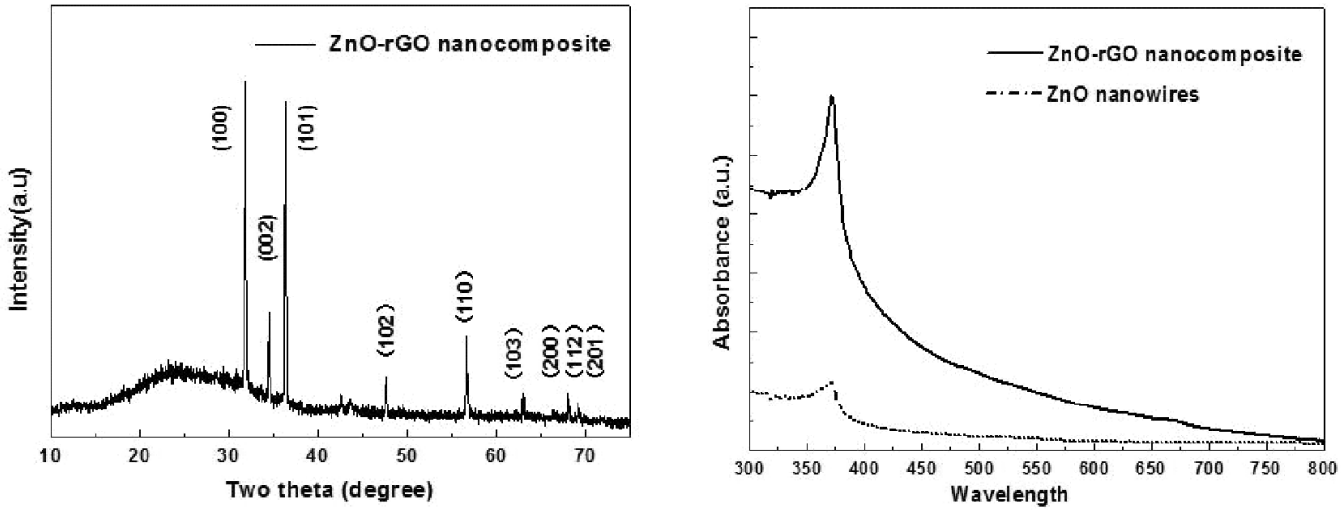

Figure 2: (a) XRD patterns of ZnO-rGO nanocomposite. (b) UV-vis absorption spectra of ZnO NWs and ZnO-rGO nanocomposite

Fig. 3 (a) shows the I-V curves of the photoelectric sensitive structure based on ZnO NWs with a low bias voltage. As can been seen from the curves, the figure of current based on ZnO nanowires was greatly increased when the white light was turned on. Moreover, the figure of current under white irradiation was obviously larger than that under UV irradiation. Fig. 3 (b) shows the current based on ZnO-rGO nanocomposite structure, whose figure was dramatically increased when the white light was turned on. The photocurrent of detector based on ZnO-rGO nanocomposite under white irradiation is nearly twice as large as its current at 1 basing voltage under UV irradiation. Compared with ZnO NWs structure under white irradiation, the current based on ZnO-rGO nanocomposite under white irradiation is close to one order of magnitude greater than its counterpart based on ZnO nanowires at 1 basing voltage.

Fig. 4 (a) shows the time dependence of photocurrent of the devices based on ZnO and ZnO-rGO nanocomposite when switching on and off the light illumination. With the white light turned on, the photocurrent of pure ZnO and ZnO-rGO nanocomposite rapidly increased to a certain value and then gradually became saturated. Then, the photocurrent decreased slowly and recovered to an initial when the light was turned off. The response

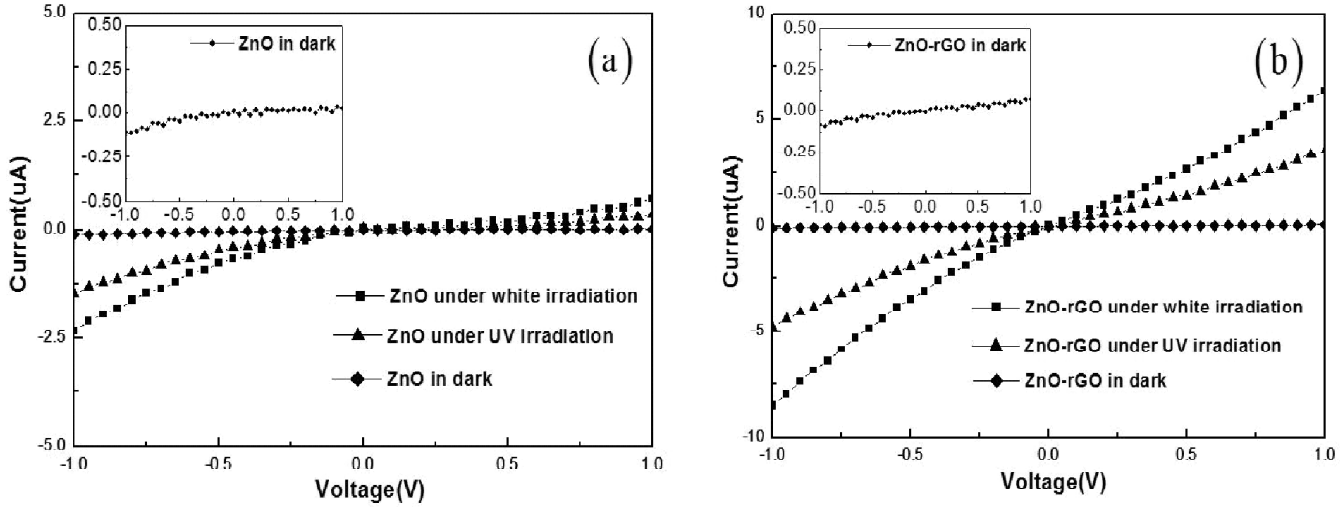

Figure 3: (a) I-V characteristics of the device based on ZnO NWs. Higher inset: the amplified I–V characteristics of ZnO device in dark. (b) I-V characteristics of the device based on ZnO-rGO nanocomposite. Higher inset: the amplified I–V characteristics of ZnO-rGO in dark

time of photocurrent rose to the half of their peak figure in 30 s for ZnO-rGO device and drops to the half of peak figure in 60 s. The higher inset shows the reproducibility of the device with the white light at 1 basing voltage under white light illumination. The recovery abilities of photocurrent are not reduced for four cycles, which indicates that the detectors based on ZnO or ZnO-rGO nanocomposite are characterized by an excellent stability and reproducibility.

Fig. 4 (b) shows the schematic diagram of sensitive device based on ZnO-rGO nanocomposite under visible illumination. When the device of ZnO-rGO nanocomposite is exposed to white light irradiation, the electrons will transfer from valence band to conduction band in ZnO nanowires. The rGO nanosheets constitute a conductive pathway in the ZnO framework as an easy passage route for transportation of charge carriers [21,22]. The separated electrons and holes under the external electric field will produce a fast photoelectric response. The results imply that photogenerated carriers of device based on ZnO-rGO nanocomposite can be easily seperated and then collected by electrodes. The photocurrent will be dramatically increased by adding rGO in the ZnO framework. The nanostructure based on ZnO-rGO nanocomposite with facile fabrication may have a great potential in visible device applications.

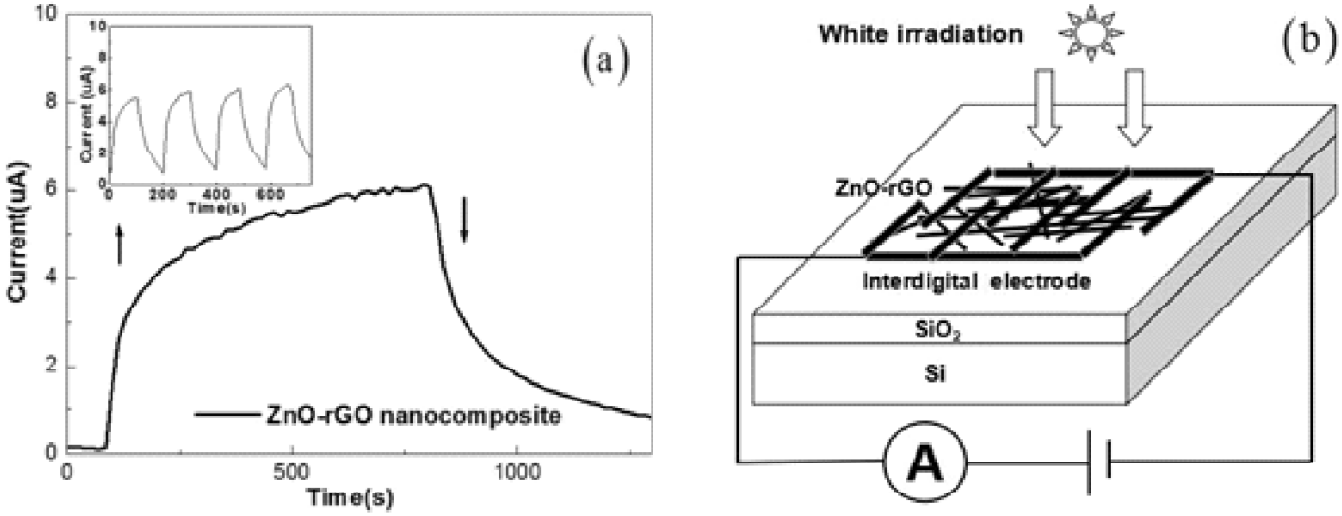

Figure 4: (a) Photocurrent versus time of the device based on ZnO-rGO nanocomposite with switching on/off the white light illumination. Higher inset: the reproducibility of the devices at 1 basing voltage under the dark and visible illumination.The bias applied on the electrodes is 1V. (b) The schematic diagram of the sensitive device based on ZnO-rGO nanocomposite under visible illumination.

4. CONCLUSION

In this research, the ZnO-rGO nanocomposite was prepared by chemical vapor deposition (CVD) as well as a microfabrication procedure. The device based on ZnO-rGO nanocomposite under white light irradiation produced a tremendous enhancement by application of a 1V bias. Meanwhile, the ZnO-rGO nanocomposite also exhibits a good photoresponse repeatability over on–off cycles of white light source. This result demonstrates that the ZnO combining with rGO can promote the separation of the electrons and holes and leads to a larger current in ZnO-rGO nanocomposite. The findings may highlight the potential visible application of the ZnO-rGO nanocomposite for new photoelectric devices.

ACKNOWLEDGEMENTS

The authors gratefully acknowledge Shanghai Funds for young college teachers (ZZSDJ15009). Scientific Research Foundation of Shanghai Dian Ji University (No. 14QD38).

REFERENCES

1. L. Sun, F. Banhart, A. V. Krasheninnikov, J. A. Rodríguez-manzo, M. Terrones, Science 2006; 312:1199.

2. C. Liu, J. A. Zapien, Y. Yao, X. Meng, C. Lee, S. Fan, Y. Lifshitz, and S. T. Lee, Adv. Mater. 2003;15:838.
3. X. J. Yang, X. Y. Miao, X. L. Xu, C. M. Xu, J. Xu, T. H. Liu, Optical Materials 2005;27:1602.
4. L. Peng, J. L. Zhai, D. J. Wang, Y. Zhang, P. Wang, Q. D. Zhao, T.F. Xie, Sens. Actuators B 148 (2010) 66–73.
5. Y. N. He, W. Zhang, S.C. Zhang, X. Kang, W.B. Peng, Y. L. Xu, Actuators A 181 (2012) 6–12.
6. N. G. N. D.J. Riler, Phys. Status SolidiA 205 (2008) 2351–2354.
7. P. X. Gao, Y. Ding, W. J. Mai, W.L. Hughes, C.S. Lao, Z.L. Wang, Science 309 (2005)1700–1704.
8. T. Xu , L. Zhang, H. Cheng , Y. Zhu, Appl Catal B 101(3) (2011) 382–387.
9. J. Zhou, Y. Gu, Y. Hu, W. Mai, P. H. Yeh, G. Bao, A. K. Sood, and Z. L. Wang, Appl. Phys. Lett. 94 (2009) 191103.
10. G. Cheng, X. Wu, B. Liu, B. Li, X. Zhang, and Z. Du, Appl. Phys. Lett. (2011) 99, 203105.
11. H.C. Qin, W.Y. Li, Y.J. Xia, T. He, ACS Appl. Mater. Interfaces 2011:3:3152-3156.
12. K. Woan, G. Pyrgiotakis, W. Sigmund, Adv. Mater. 21 (2009) 2233–2239.
13. H. Zhang, X.J. Lv, Y.M. Li, Y. Wang, J.H. Li, ACS Nano 2010;4:380-386.
14. Dali Shao, XiangSun, MingXie, HongtaoSun, FengyuanLu, ShaylaSawyer, Materials Letters 2013;112:165-168.
15. Huynh Ngoc Tien, Van Hoang Luan, Seung Hyun Hur, Chemical Engineering Journal 2013:229:126-133.
16. R. Kumar, R.K. Singh, J. Singh, R.S. Tiwari, O.N. Srivastava, Synthesis, J. Alloys Comp. 2012;526:129–134.
17. N. Hu, L. Meng, R. Gao, Y. Wang, J. Chai, Z. Yang, E. S. W. Kong and Y. Zhang, Nano-Micro Lett., 2011; 3: 215.
18. Y. J. Su, X. L. Lu, M. M. Xie, H. J. Geng, H. W, Z.Y, Y. F. Zhang, Nanoscale 2013;5:8889.
19. J. Wang, L. M. Wei, L. Y. Zhang, Y. F. Zhang, *et al*. Journal of Materials Chemistry 2012;22:20038-20047.
20. Xiaoliang Ye, Hong Liu, Ming Li, Yafei Zhang, Materials Letters 150 (2015) 126–129.
21. L. Guo, H. Zhang, D.X. Zhao, B.H. Li, Z.Z. Zhang, D.Z. Shen, Sens. Actuators B 2012; 166 : 12–16.
22. M.S. Kim, J.H. Han, D.H. Lee, E.H. Lee, S.G. Park, Microelectron. Eng. 2012; 97: 130–133.